ACS Catalysis

Research Article

pubs.acs.org/acscatalysis

Evidence for Iron Nanoparticles Catalyzing the Rapid Dehydrogenation of Ammonia-Borane

Jessica F. Sonnenberg and Robert H. Morris*

Davenport Laboratories, Department of Chemistry, University of Toronto, 80 St. George Street, Toronto, Ontario M5S 3H6, Canada

Supporting Information

ABSTRACT: A series of precatalysts of the general formula $[Fe(NCMe)(L)(PPh_2C_6H_4CH{=}NCHR\text{-})_2][BF_4]_2$ (where L = CO or NCMe, and R = Ph or H) were tested for the dehydrogenation of amine-boranes. They have already been used in our lab for the transfer hydrogenation or direct hydrogenation of ketones and the oxidative kinetic resolution of alcohols. We compared a series of sterically- (R = H or Ph) and electronically- (L = NCMe or CO) varied precatalysts in both protic and aprotic solvents for the release of hydrogen from ammonia-borane (AB) and studied the products by NMR. At room temperature in tetrahydrofuran (THF) we optimized our systems, and achieved maximum turnover frequencies (TOF) of up to 3.66 H_2/sec and 1.8 total H_2 equivalents, and in isopropanol we were able to release a maximum of 2.9 equiv of H_2 and reuse some of our catalytic systems. In previous mechanistic studies we provided strong evidence that the active species during transfer hydrogenation (TH) and oxidation catalysis are zerovalent iron nanoparticles formed by the reduction of the Fe-PNNP precatalysts with base. To probe the dehydrogenation active species we successfully show comparable activity between preformed catalysts, and those generated in situ using commercially available Fe^{2+} sources and substoichiometric amounts of PNNP ligand. This result, when paired with transmission electron microscope images of ∼4 nm iron nanoparticles of reaction solutions provide evidence that the highly active systems studied are heterogeneous in nature. This would be the first report of iron nanoparticles catalyzing H_2 evolution from AB in nonprotic solvents. We also report the evolution of hydrogen from dimethylamine-borane and the resultant product mixtures using the same catalyst series.

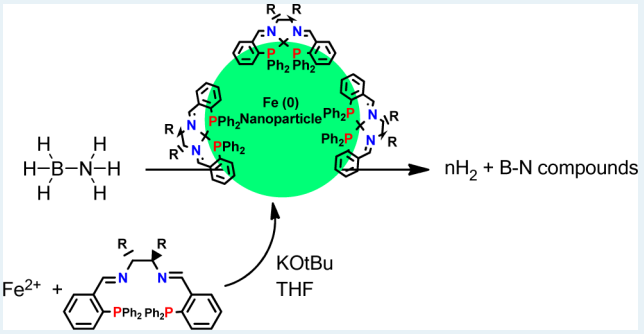

KEYWORDS: *iron nanoparticles, ammonia-borane dehydrogenation, B−N polymers, heterogeneous, hydrogen evolution, catalytic profile, electron microscopy*

INTRODUCTION

The transition from high carbon content liquid and solid based fuels into gas based fuels for energy applications is of growing economic importance.[1] Emerging as the ideal candidate as a clean, lightweight, and high energy density fuel is hydrogen gas.[2] Among the major challenges in the use of hydrogen is its storage and production in an efficient and "green" way.[3] A potential candidate to solve this problem is ammonia borane, $NH_3{\cdot}BH_3$ (AB), which has a total hydrogen content of 19.6 wt %, or 6.5 and 13.1 wt % for the first and second equivalent of hydrogen released.[4,5] When analyzing catalysts for such a transformation it is important to study not only the number of equivalents of H_2 released but also the reaction conditions and type of B/N containing products formed.[4,6,7] There are a significant number of catalytic systems in the literature employing water and protic solvents for the dehydrogenation/hydrolysis of AB,[4] and although larger numbers of equivalents of H_2 are evolved, the formation of strong B−O bonds precludes their use in industry as the wastes are not recyclable.[8] It is therefore important to generate catalysts that operate in nonprotic solvents such as tetrahydrofuran (THF), aromatic solvents or glyme, as the typical products contain B−N bonds which can be used to regenerate AB.[8]

There are several homogeneous systems in the literature based on precious metal catalysts,[9−18] as well as more abundant metals such as titanium,[19] nickel,[20,21] and iron,[7,22] and group 6 metal carbonyls[23] that have been used as dehydrogenation catalysts. Heterogeneous catalysts have also been studied, primarily using precious metal catalysts,[24−28] although there are reports using nickel heterogeneous catalysts[29] for the dehydrogenation of amine-boranes, including ammonia-borane. In the field of iron catalysts for this transformation a few key discoveries stand out as stepping stones. First was the work by Xu et al.[30] who reduced $Fe(SO_4)$ to generate stable, 3 nm, zerovalent iron nanoparticles (FeNPs) that were able to evolve 3 equiv of hydrogen from ammonia-borane in water at room temperature. Their catalyst was stable under air and magnetically recyclable; however, it was only used for hydrolysis of AB to generate borates, not B−N

Received: February 13, 2013
Revised: April 5, 2013
Published: April 9, 2013

polymers or oligomers. The next key example was the use of $[\{CpFe(CO)_2\}_2]$ under photoirradiation to dehydrogenate amine-boranes by Manners et al.[22] wherein they also determined the identity of several of the products and intermediates during the reaction. Baker et al.[7] used iron systems with phosphine and amido ligands to evolve 1−2 equiv of H_2 and generate $(BH_2NH_2)_n$ and $(BHNH)_n$ oligomers. Their active systems are hypothesized to be based on zerovalent iron systems stabilized by ligands. There is therefore a vacancy in the literature in terms of using defined heterogeneous iron catalyst for the dehydrogenation of amine-boranes to yield B−N polymers and oligomers.

Our group has reported the synthesis of iron complexes of the general formula $[Fe(NCMe)(L)(PNNP)][BF_4]_2$ where L = NCMe or CO and PNNP = $(PPh_2C_6H_4CH{=}NCHR\text{-})_2$, as depicted in Figure 1, which have been shown to be highly

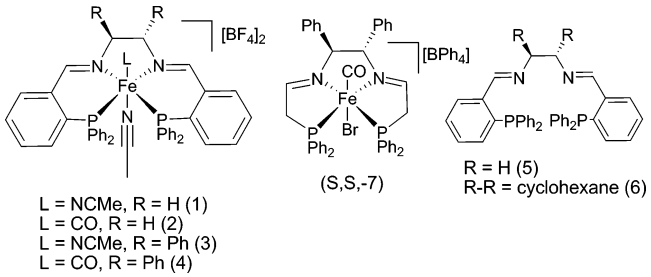

Figure 1. Precatalyst structures for systems investigated for ammonia-borane dehydrogenation reactions including ligands tested.

active for direct H_2-hydrogenation of ketones[31] (L = NCMe) and for the transfer hydrogenation (TH) of ketones using isopropanol (iPrOH) as the hydrogen source[32] (L = CO). Upon further investigation of the catalyst during TH we proposed that the active catalytic species are zerovalent iron nanoparticles (FeNPs). This proposition was based on density functional theory (DFT) support for a low energy pathway for the formation of iron(0)[33] as well as extensive poisoning, imaging, and in operando experiments.[34] The FeNPs are proposed to be a zerovalent iron core, coated in PNNP ligand, able to bind substrate to active sites and transfer a proton and hydride equivalent. These nanoparticle catalysts were further probed and shown to be active for the reverse process; oxidative kinetic resolution of aromatic alcohols to enantio-enriched alcohols and ketones, and their heterogeneity was similarly probed.[35] These precatalysts with the general formula $[Fe(NCMe)(L)(PNNP)][BF_4]_2$ have therefore proven themselves to be quite versatile in terms of their chemistry with hydrogen, and we were therefore interested in probing their ability to act as hydrogen evolving catalysts in the dehydrogenation of ammonia-borane, as depicted in Scheme 1 for our optimized reaction conditions. The use of alcohol oxidation/reduction catalysts for amine-borane dehydrogenation has been previously reported using $Ru(PN)_2$ catalysts[11] and were found to be quite active in terms of both rates and extent of H_2 release.

EXPERIMENTAL SECTION

General Procedures. All preparations, manipulations and catalysis were carried out under argon or nitrogen atmosphere using standard Schlenk line and drybox techniques. Dry and oxygen-free solvents were distilled and dried using the appropriate drying agents. NMR solvents were purchased from Aldrich and degassed and dried over activated molecular sieves. All other reagents were purchased from various commercial sources and used without further purification. NMR spectra were recorded using a Bruker 400 and a Varian 400 spectrometer to determine ^1H (400 MHz), ^{11}B (128 MHz), and $^{31}P\{^1H\}$ (161 MHz) shifts.

Electron microscopy imaging was carried out at the Department of Pathology and Laboratory Medicine in the Joseph and Wolf Lebovic Health Complex at Mount Sinai Hospital in collaboration with Dr. Doug Holmyard on a Tecnai-20 using a GIF2000 energy filter. Samples were placed on an ultrathin carbon film supported by a lacey carbon film on a 400 mesh copper grid.

Syntheses. Precatalysts $[Fe(NCMe)_2(P_2N_2en)][BF_4]_2$ (**1**), $[Fe(CO)(NCMe)(P_2N_2en)][BF_4]_2$ (**2**), $[Fe(NCMe)_2(P_2N_2dpen)][BF_4]_2$ (**R,R-3**) and $[Fe(CO)(NCMe)(P_2N_2dpen)][BF_4]_2$ (**R,R-4**) and ligands $\{(PPh_2(o\text{-}C_6H_4)CH{=}NHCH_2-)_2\}$: (P_2N_2en) (**5**) and (R,R)-$\{(PPh_2(o\text{-}C_6H_4)CH{=}NH(C_6H_{10})NH{=}CH(o\text{-}C_6H_4)PPh_2)\}$: (P_2N_2cy) (**R,R-6**) have been prepared and characterized previously.[31,32,36,37] Precatalyst (S,S)-$[Fe(CO)(Br)(PPh_2CH_2CH{=}NHCHPh\text{-})_2][BPh_4]$ (**S,S-7**) has been prepared and characterized previously.[38]

Catalysis. In an argon filled glovebox, precatalyst and ammonia-borane (AB) were added to a 25 mL two-neck round-bottom flask which was sealed with a rubber septum and a 10 mL dry-addition flask containing KOtBu. The sealed system was removed from the glovebox and submerged in a bath at a set, regulated temperature before solvent was added to the flask and stirred for 10 min. A cannula needle was used to pierce the septum and monitor the evolution of gas into an upturned 50 mL buret filled with water. To start the reaction, the dry-addition flask was tilted, and base was added to the reaction, which was stirred vigorously. Hydrogen production was measured in terms of volume displacement of water in the buret as a measure of time. All catalytic results were reproduced in triplicate to ensure consistency.

RESULTS AND DISCUSSION

AB Dehydrogenation with Precatalysts (1−4) in Protic Solvents. Following Xu et al.'s work[30] on the hydrolysis of AB using 3 nm FeNPs, we were interested in applying our FeNP TH precatalysts (**2**) and (**4**) to the dehydrogenation of AB. The optimized method for the formation of FeNPs for our previously reported transfer hydrogenation catalysis was the reaction of an excess of KOtBu in iPrOH with precatalyst (**2**) or (**4**) before the addition of substrate. Therefore, for the dehydrogenation of AB we first tested our precatalysts in protic solvents using a slightly modified technique as outlined in the Experimental Section. Using 2.5 mol % precatalyst at 22 °C, (**1**−**4**) were tested as

Scheme 1. Generalized Reaction Scheme and Product Distribution for Optimized Catalytic System

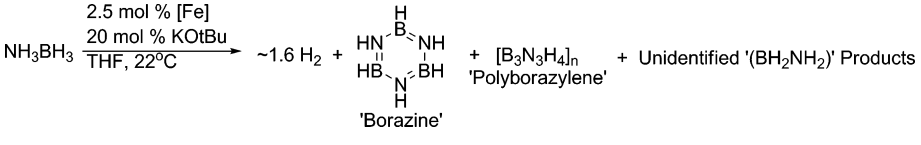

dx.doi.org/10.1021/cs400115p | ACS Catal. 2013, 3, 1092−1102

Table 1. Reaction Conditions for All Catalytic Hydrogen Evolution Reactions Using Iron Catalysts

entry	catalyst (mg, mmol)	other (mg, mmol)	H_2 source (mg, mmol)	KO*t*Bu (mg, mmol)	C:B:S[b]	solvent (mL, mmol)	*T* (°C)	equiv. H_2 1 min/1 h
1	(**1**) (7, 0.0076)	N/A	AB (10, 0.32)	(8, 0.071)[a]	1:9:42	iPrOH (5, 65)	22	0.93/2.50
2	(**2**) (7, 0.0077)	N/A	AB (10, 0.32)	(8, 0.071)[a]	1:9:42	iPrOH (5, 65)	22	0.15/2.58
3	(**R,R-3**) (9, 0.0084)	N/A	AB (10, 0.32)	(8, 0.071)[a]	1:8:38	iPrOH (5, 65)	22	0.59/2.89
4	(**R,R-4**) (9, 0.0085)	N/A	AB (10, 0.32)	(8, 0.071)[a]	1:8:38	iPrOH (5, 65)	22	0.20/2.90
5	$[Fe(H_2O)_6][BF_4]_2$ (5, 0.015)	(**5**) (5, 0.0083)	AB (10, 0.32)	(10, 0.089)[a]	1:6:21	iPrOH (5, 65)	22	0.17/1.02
6	(**1**) (7, 0.0076)	N/A	AB (10, 0.32)	(8, 0.071)[a]	1:9:42	THF (5, 62)	22	1.13/1.60
7	(**1**) (7, 0.0076)	N/A	AB (10, 0.32)	(8, 0.071)[a]	1:9:42	THF (5, 62)	2	0.95/1.40
8	(**1**) (7, 0.0076)	CO headspace	AB (10, 0.32)	(8, 0.071)[a]	1:9:42	THF (5, 62)	22	0.05/0.09
9	(**1**) (5, 0.0055)	N/A	AB (20, 0.64)	(6, 0.053)[a]	1:9:42	THF (5, 62)	22	1.0/1.22
10	(**2**) (7, 0.0077)	N/A	AB (10, 0.32)	(8, 0.071)[a]	1:9:42	THF (5, 62)	22	0.48/1.26
11	(**R,R-3**) (9, 0.0084)	N/A	AB (10, 0.32)	(8, 0.071)[a]	1:8:38	THF (5, 62)	22	1.14/1.71
12	(**R,R-4**) (9, 0.0085)	N/A	AB (10, 0.32)	(8, 0.071)[a]	1:8:38	THF (5, 62)	22	0.80/1.44
13	$[Fe(H_2O)_6][BF_4]_2$ (5, 0.015)	(**5**) (5, 0.0083)	AB (10, 0.32)	(10, 0.089)[a]	1:6:21	THF (5, 62)	22	0.62/1.61
14	$[Fe(H_2O)_6][BF_4]_2$ (5, 0.015)	(**R,R-6**) (5, 0.0083)	AB (10, 0.32)	(10, 0.089)[a]	1:6:21	THF (5, 62)	22	1.08/1.43
15	(**S,S-7**) (9, 0.0081)	N/A	AB (10, 0.32)	(8, 0.071)[a]	1:9:40	THF (5, 62)	22	0.28/0.71
16	$FeBr_2$ (2.75, 0.013)	N/A	AB (10, 0.32)	(10, 0.089)[a]	1:7:25	THF (5, 62)	22	0.24/0.67
17	$FeBr_2$ (2.75, 0.013)	(**5**) (5, 0.0083)	AB (10, 0.32)	(10, 0.089)[a]	1:7:25	THF (5, 62)	22	1.01/1.59
18	$FeBr_2$ (2.75, 0.013)	(**5**) (10, 0.016)	AB (10, 0.32)	(10, 0.089)[a]	1:7:25	THF (5, 62)	22	1.03/1.53
19	$FeBr_2$ (2.75, 0.013)	(**5**) (2.5, 0.004)	AB (10, 0.32)	(10, 0.089)[a]	1:7:25	THF (5, 62)	22	1.06/1.50
20	$FeBr_2$ (2.75, 0.013)	(**5**) (1, 0.002)	AB (10, 0.32)	(10, 0.089)[a]	1:7:25	THF (5, 62)	22	1.11/1.58
21	$FeBr_2$ (2.75, 0.013)	(**5**) (5, 0.0083)	AB (10, 0.32)	(10, 0.089)[a]	1:7:25	THF (5, 62)	2	0.87/1.24
22	(**1**) (7, 0.0076)	N/A	AB (10, 0.32)	(8, 0.071)[a]	1:9:42	diglyme (5, 35)	22	1.06/1.44
23	(**2**) (7, 0.0077)	N/A	AB (10, 0.32)	(8, 0.071)[a]	1:9:42	diglyme (5, 35)	22	0.43/1.11
24	(**1**) (7, 0.0076)	N/A	Me_2AB (20, 0.34)	(8, 0.071)[a]	1:9:45	THF (5, 62)	22	0.63/0.98
25	(**2**) (7, 0.0077)	N/A	Me_2AB (20, 0.34)	(8, 0.071)[a]	1:9:45	THF (5, 62)	22	0.44/0.96
26	(**1**) (7, 0.0076)	N/A	AB (10, 0.32)	(16, 0.14)[a]	1:18:42	THF (5, 62)	22	1.33/1.83
27	(**1**) (7, 0.0077)	N/A	AB (10, 0.32)	(4, 0.035)[a]	1:5:42	THF (5, 62)	22	1.00/1.25
28	(**1**) (7, 0.0077)	N/A	AB (10, 0.32)	(37, 0.33)[a]	1:43:42	THF (5, 62)	22	1.17/1.66
29	(**1**) (7, 0.0077)	N/A	AB (10, 0.32)	0[c]	1:10[c]:42	THF (5, 62)	22	0.99/1.22
30	$FeBr_2$ (1.75, 0.008)	(**5**) (3.0, 0.005)	AB (10, 0.32)	(8, 0.071)[a]	1:9:40	THF (5, 62)	22	0.98/1.43
31	$FeBr_2$ (1.75, 0.008)	(**5**) (3.0, 0.005)	AB (10, 0.32)	(8, 0.071)[a]	1:9:40	diglyme (5, 35)	22	1.11/1.39
32	(**1**) (7, 0.0077)	N/A	AB (5, 0.16)	(6, 0.053)	1:7:21	THF (5, 62)	28[d]	N/A
33	$FeBr_2$ (2.75, 0.013)	(**5**) (2.5, 0.04)	AB (7, 0.22)	(7, 0.062)	1:5:17	THF (5, 62)	28[d]	N/A

[a]When the dry-addition flask is tilted and base added, ~1 mg of KO*t*Bu remains trapped in the flask, hence why an excess was always added. [b]C:B:S = molar ratio of catalyst:base:substrate/H_2 source. [c]Used NaOiPr (6 mg, 0.073 mmol). [d]Reactions done in a vial in an argon glovebox - solutions used for TEM imaging.

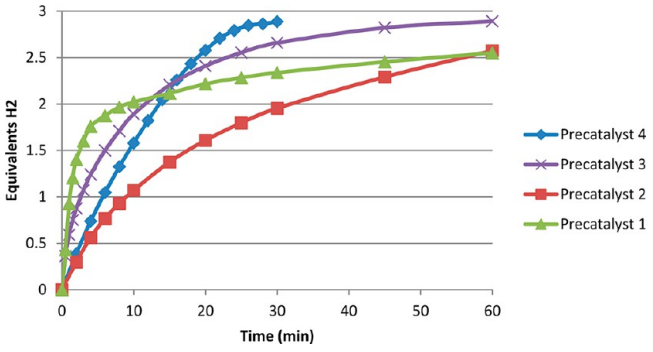

Figure 2. Catalytic dehydrogenation of AB (10 mg, 0.32 mmol) in 5 mL of iPrOH at 22 °C using 2.5 mol % Fe and 20 mol % KOtBu. Fe:AB:KOtBu = 1:40:8.

outlined in entries 1−4 of Table 1 yielding the results shown in Figure 2. Several observations can be made from the plot; all four precatalysts are active and yield >2.5 equiv of H_2 in an hour. For TH, a 6−8 min induction period was observed for the formation of the FeNPs, whereas none of the reaction profiles in Figure 2 show this. An induction period is often indicative of heterogeneous catalysis;[39,40] however, Xu et al. also reported no induction period for their in situ generated system. Also of note, the bis-MeCN complexes (**1**) and (**3**) show a more rapid initial rate and a more rapid deactivation (plots level off at a lower number of equivalents of H_2) than the corresponding MeCN-trans-CO complexes (**2**) and (**4**). The reason for this difference is unclear, but it would suggest that the catalysts derived from the bis-MeCN precatalysts have more active sites available because of the increased lability of MeCN versus CO. This increased lability would result in more rapid initial rates, and more ready deactivation. (**3**) and (**4**) are slightly more active than (**1**) and (**2**) indicating that the bulkier phenyl groups in the PNNP ligand are better stabilizers of the active species than the achiral complex with protons in the PNNP backbone of the ligand. ^{11}B NMR of active solutions show a singlet at 18.2 ppm, corresponding to $B(OiPr)_3$ as would be expected for reactions in iPrOH.

To test the reuse of our catalytic systems we added another 40 equiv of AB to the reaction mixtures after 30 min. Upon addition, (**1**−**3**) released ~1 equiv of H_2 within 2 h, indicating that the catalyst was significantly deactivated. Interestingly, addition of a second batch of AB to catalysis with (**4**) resulted in

dx.doi.org/10.1021/cs400115p | *ACS Catal.* 2013, 3, 1092−1102

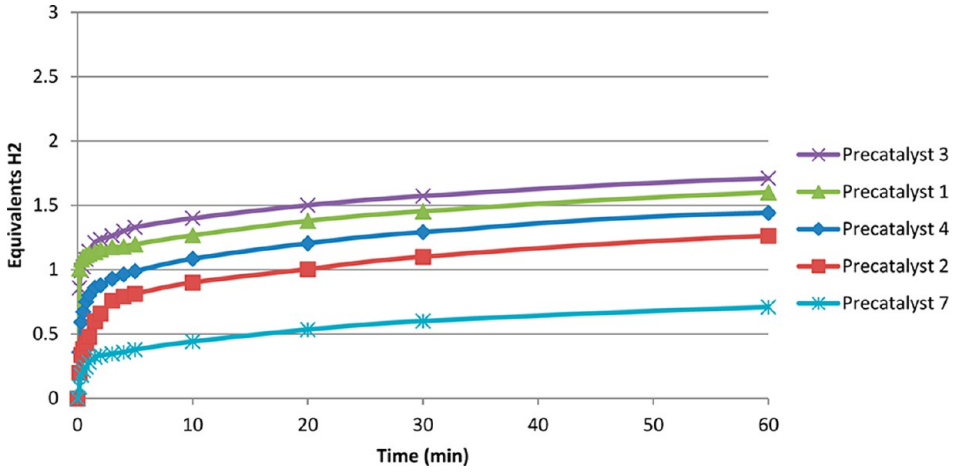

Figure 3. Catalytic dehydrogenation of AB (10 mg, 0.32 mmol) in 5 mL of THF at 22 °C using 2.5 mol % Fe and 20 mol % KOtBu.

2.4 equiv of H_2 released in 40 min before deactivation occurred, and further recycling by addition of more AB was unsuccessful. This would suggest that the active species derived from (**4**) is slightly better stabilized than the species derived from (**1**−**3**), but that all species are not good candidates for multiple recycles, unlike the species studied by Xu et al.[30]

We also explored the use of water and methanol as potential solvents. Only minimal activity was observed using (**2**) and (**4**) with MeOH as the solvent, and no activity was observed using (**1**−**4**) with water as the solvent. There is no hydrogen evolution if any component (Fe, base, AB) is missing.

AB Dehydrogenation with Precatalysts (1−4, 7) in Non-Protic Solvents. We were interested in using our catalysts to generate B−N polymers and oligomers from AB using nonprotic solvents such as THF and glyme. Using the same catalytic conditions as outlined with iPrOH, we tested THF as a solvent with (**1**−**4**) as outlined by entries 6, 10−12 of Table 1, and the results are shown in Figure 3. All four systems are highly active, releasing half an equivalent of H_2 within seconds and a full equivalent in under a minute in the case of (**1**) and (**3**) and in less than 20 min for (**2**) and (**4**). Similar to the case in iPrOH, the bis-MeCN catalysts are faster at H_2 evolution than their MeCN-trans-CO counterparts. MeCN may be a more labile ligand than CO on iron nanoparticles, yielding a less stable species. This might yield a larger number of active sites in either a homogeneous or heterogeneous catalyst, and thus increase catalytic activity. This was not the case for TH as the one carbonyl ligand was necessary to promote catalytic activity.[32] (**3**) and (**4**) are slightly more active than (**1**) and (**2**) respectively, again suggesting the added stabilization of the catalysts containing the bulkier diphenyl backbone in the PNNP ligand versus the achiral PNNP which contains only protons in the backbone. All of the catalytic systems also show a similar reaction profile, whereby there is very rapid catalytic activity in the first 3 min, followed by a significant decrease in rate resulting in very slow H_2 evolution for the proceeding hour. This reaction profile for dehydrogenation of amine-boranes is fairly common, as has been seen for both heterogeneous NP catalysis[25] as well as homogeneous catalysis, specifically the $Ru(PN)_2$ alcohol oxidation/reduction catalysts tested by Blaquiere et al.[11] There are two possible explanations for this rapid decrease in activity; first, that all of the AB has been consumed and converted into the most stable product. This is not the case because AB is still present according to ^{11}B NMR (vide infra) and because addition of more AB yields no further H_2 evolution. This therefore indicates that the cause for the rate decrease is deactivation of the catalyst. Baker et al. observed that, upon catalyst deactivation with their system, a black residue of bulk iron was formed;[7] however this is not observed with our systems. They also observed protonation of their amide ligands and formation of P−B adducts with their phosphine ligands, which we did not observe in the ^{11}B NMR. Instead the primary species observed with $^{31}P\{^1H\}$ NMR is decoordinated PNNP ligand at −16 ppm. A similar spectrum was observed with the activated solution in TH[33] when some of the PNNP ligand decoordinated to allow for formation of FeNPs. The release of PNNP ligand and the observation that no bulk iron is released supports that FeNPs are forming during catalysis and that deactivation involves blocking of active sites on the NP surface, potentially by reactive B−N compounds. Further discussion of deactivation modes on iron will be discussed vide infra. Also depicted in Figure 3 is the reaction profile using precatalyst (S,S)-[Fe(CO)(Br)(PPh_2CH_2CH═NHCHPh-)$_2$][BPh_4] (**7**) (entry 15 of Table 1). This precatalyst is a highly active TH system also developed in our group[38,41] that was recently studied mechanistically[42] and determined to likely operate via a homogeneous mechanism, as there are no low energy pathways leading to Fe(0).[43] This system is much less active than systems (**1**−**4**), supporting that the systems operate via different mechanisms for the dehydrogenation of AB, also suggesting that precatalysts (**1**−**4**) may generate FeNPs during catalysis.

$^{11}B\{^1H\}$ NMR spectra of the activated solutions using (**1**) contained peaks for some unreacted AB and four major species at 20.3, 24.3, 27.8, and 30.9 ppm. Upon coupling to protons, the peaks at 27.8 and 30.9 split into doublets with coupling constants of 137 and 132 Hz respectively, indicating two different B−H groups and two different unprotonated boron sites are present. The peak at 30.9 ppm is assigned to be borazine,[9] and the remaining coupled and uncoupled boron species are tentatively assigned as polyborazylene (PB) and short chain B−N oligomers or partially cross-linked polyborazylene which could not be isolated or identified further. ^{11}B NMR of the activated solutions using (**2**) also contained unreacted AB, a triplet at −10 ppm for cyclotriborazane (CTB)[7,9] and two doublets at 30.9 and 27.9 as observed with (**1**). This correlates with the fact that (**1**) generates more H_2 than (**2**), in agreement with the formation of some PB versus CTB.

dx.doi.org/10.1021/cs400115p | *ACS Catal.* 2013, 3, 1092−1102

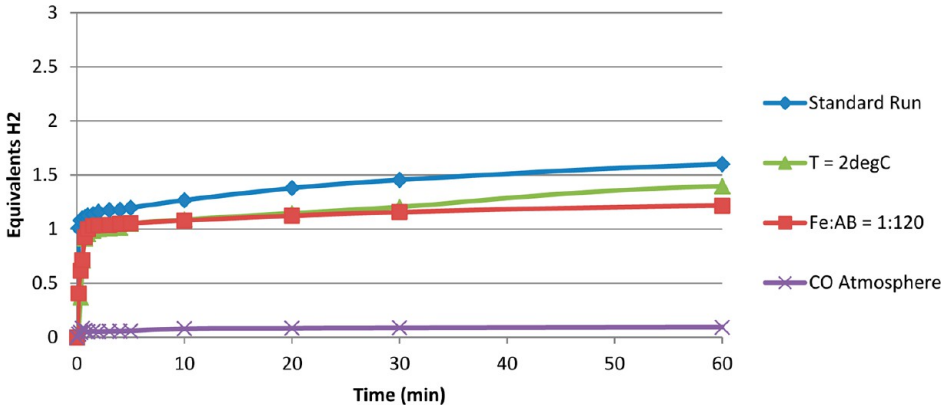

Figure 4. Catalytic dehydrogenation of AB. Standard Run: AB (10 mg, 0.32 mmol) in 5 mL of THF at 22 °C using 2.5 mol % Precatalyst (**1**) and 20 mol % KOtBu, Fe:AB:KOtBu = 1:40:8. Variations from standard conditions as listed in legend.

The difference in activity of (**1**) and (**2**) versus (**3**) and (**4**) was small, and therefore the use of the more expensive, chiral catalysts bearing the diphenyl backbone was discontinued and further experiments were only conducted using (**1**) and (**2**).

Because of the highly solvent dependent nature of these systems whereby there is no hydrogen evolution in water, slow but continuous evolution in iPrOH and rapid activity in THF, we also tested diglyme as a dehydrogenation solvent (Entries 22−23, Table 1). Reaction profiles using both (**1**) and (**2**) in THF were compared to profiles of reactions done in diglyme, and the plots were the same, within error. This suggests that the same active species is generated in both solvents.

Effect of Varying Conditions of AB Dehydrogenation with Precatalyst (1). Following optimizations of the solvent and precatalyst, we chose to further evaluate (**1**) under varying conditions to probe its robustness. We first probed the catalytic system for its temperature dependence. Standard reactions are run at 22 °C, so we tested the activity of the system when it was precooled using an ice bath (entry 7, Table 1) The reaction profile is depicted in Figure 4 and shows that although the activity is decreased slightly when compared to runs at 22 °C, the system is still quite active, evolving 1 equiv of H_2 in 2 min, and 1.4 equiv in an hour before deactivating, compared to 1 equiv of H_2 in less than 30 s and 1.6 equiv in an hour for the reaction at 22 °C. The decrease in initial rate can be attributed to slower activation at lower temperatures, but the overall high efficiency of the system at 2 °C reflects how unique these systems are when compared to the majority of other AB dehydrogenation catalysts that require high temperatures.[10,14,25] Because of the difference in activity observed between the bis-MeCN and MeCN-trans-CO precatalysts, we were interested in the effect CO gas would have on the activity of the catalysts (entry 8, Table 1). When reactions were run under a CO headspace instead of an argon headspace, minimal H_2 evolution was observed, as shown in Figure 4. This would suggest that either active species are forming and are immediately poisoned by CO, or CO inhibits the formation of active species. Because no initial activity is observed, it is likely that the active species do not form under these conditions. To further probe this, we attempted to poison the system after activation with a known amount of CO; however the results were inconclusive because the reaction setup employs an open system and the CO gas was rapidly purged by the evolving hydrogen.

We were also interested in testing the limits of the catalyst at much higher AB loadings to see if our systems could compare to the highly rapid ruthenium systems developed by Schneider[15] and Fagnou.[11] Using 0.83 mol % (**1**) (Fe:AB = 1:120 instead of Fe:AB = 1:40) (entry 9, Table 1) we observed the same general reaction profile, releasing 1 equiv of H_2 in under 1 min, as shown in Figure 4. Using the linear portion of the plot (the first 30 s) the turnover frequency (TOF) can be calculated:

$$\mathrm{TOF} = \frac{n_{\mathrm{H2}}}{t \times n_{\mathrm{Fe}}} = \frac{\mathrm{slope}}{n_{\mathrm{Fe}}} = 3.66\ \mathrm{s}^{-1}$$

Although the TOF is exceptionally high, the overall turnover number (TON) is only 154 H_2 per Fe because of catalyst deactivation.

Standard experiments were done using 8 equiv of KOtBu as the base, relative to iron, and we were interested in probing the dependence of catalytic activity on base and therefore ran experiments using both double (16 equiv, entry 26) and half (4 equiv, entry 27, Table 1) the amount of base, and the reaction profiles are depicted in Figure 5. As would be expected, all three profiles (standard run, and half and double KOtBu) show the same general shape with rapid initial activity followed by a significant rate decrease as the catalyst deactivates; however the initial rate with half base is slower, and the overall H_2 production varies between all three sets of experiments. The slower initial rate with 4 equiv of base versus 8 or 16 (1 equiv of H_2 in 45 s for half base versus 10 s for both 8 and 16 equiv) can be attributed to slower activation with a lower concentration of base. More surprisingly was the overall yield of H_2 achieved by varying the concentration of base; 1.83, 1.60, and 1.25 equiv of H_2 in 1 h for 16, 8, and 4 equiv of base (relative to (**1**)), respectively. Given the similar reaction profiles and same initial rates for 8 and 16 equiv of KOtBu, it would appear as though catalyst activation is occurring in all cases. It is possible that deactivation of the catalyst is minimized under the more basic conditions, as alkoxides could protect the active sites; however the exact reason is still unclear. To probe this, we thought that perhaps the base was reacting stoichiometrically with boron-containing intermediates, allowing for more equivalents to be released when more base was present. We were able to rule this out, as running the reaction with equimolar amounts of KOtBu and AB (entry 28, Table 1) we did not evolve more H_2 than with 40 mol % KOtBu. Rather, we saw a decrease in overall yield (1.66 equiv of H_2 in 1 h in comparison to 1.83), indicating that too much base has the opposite effect, and that the base dependence of this system is much more complicated. To complete our base dependence studies, we tested the use of NaOiPr, as it is both reducing and basic, albeit less basic than KOtBu. KOtBu is a very

dx.doi.org/10.1021/cs400115p | ACS Catal. 2013, 3, 1092−1102

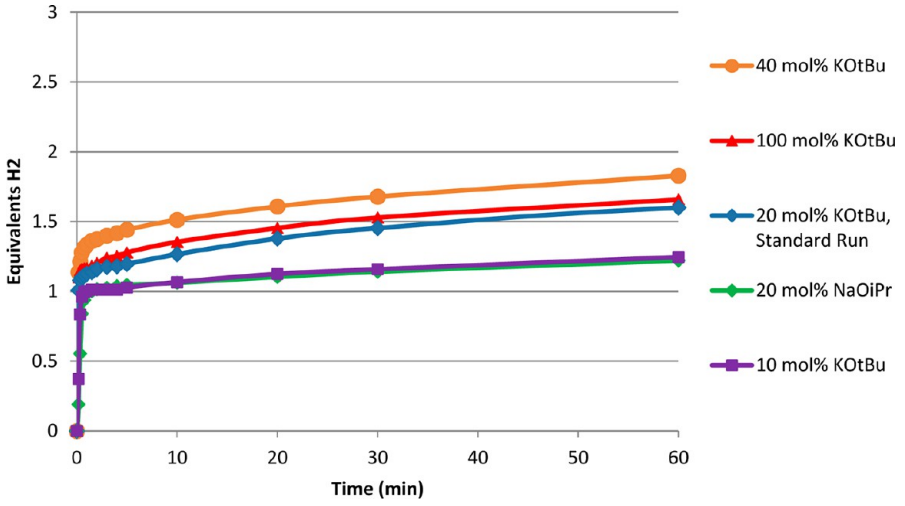

Figure 5. Catalytic dehydrogenation of AB. Standard Run: AB (10 mg, 0.32 mmol) in 5 mL of THF at 22 °C using 2.5 mol % precatalyst (**1**) and base.

strong base but is not reducing, whereas NaOiPr is a weaker base but is a moderately strong reductant. Using the standard 20 mol % NaOiPr (entry 29, Table 1) we observed that the system was much less active, in terms of both initial rates and overall H_2 evolution, as depicted by the green plot in Figure 5. Therefore reduction of iron occurs most rapidly in the presence of AB and the stronger base.

Finke has reported that the formation of nanoparticles for use in catalysis can be viewed as an autocatalytic process[44] whereby precatalyst forms active NP catalyst, which then autocatalyzes the formation of more active catalyst. From this we would expect that at very low precatalyst concentrations formation of NPs would be significantly slower and that an induction period might occur. To test the dependence of catalysis on iron concentration, we varied the concentration of (**1**) in otherwise identical reaction conditions. Precatalyst concentrations of 1.5, 0.65, and 0.15 mM were tested. 1.5 and 0.65 mM yielded similar reaction profiles with rapid initial activity followed by deactivation; however the initial rate using 0.65 mM precatalyst was approximately 75% that of the standard 1.5 mM run. Dropping the concentration of precatalyst lower to 0.15 mM yielded a completely different profile exhibiting a 10 s induction period, followed by rapid catalytic activity then deactivation. This non-first order kinetics is to be expected for NP formation as at very low iron concentrations nucleation and growth of NPs is expected to be significantly slower.

AB Dehydrogenation with In Situ Generated Catalysts. Further optimization of our catalytic systems led to an investigation of in situ generated catalysts that would preclude the necessity to first generate our FePNNP precatalysts. This involved using a one pot reaction of commercially available Fe(II) precursors, KOtBu, AB, PNNP-ligand, and solvent. We previously calculated that for the 4 nm FeNPs derived from (**2**) and (**4**) for TH that approximately 50% of the iron would be on the surface,[34] indicating that less than half of the ligand was being used. We therefore ran initial tests using Fe(II) precursors and 0.6 equiv of PNNP-ligand. $[Fe(H_2O)_6][BF_4]_2$ was tested with ligand (**5**) from Figure 1, the same PNNP ligand of (**1**) and (**2**), in iPrOH (entry 5) and THF (entry 13, Table 1) for AB dehydrogenation using 4 mol % Fe (relative to AB). In iPrOH the reaction rate was much slower than the preformed catalysts, yielding only 1 equiv of H_2 in just under an hour before the system deactivated. In THF, the in situ generated catalyst showed comparable activity in terms of initial rates and overall H_2 generation to reactions using (**1**), at a lower AB loading, suggesting that the same active species is being formed. To further investigate ligand effects we synthesized bulkier and more basic PNNP ligand (**6**) as shown in Figure 1 which contains a cyclohexyl diamine backbone (entry 14, Table 1) and compared activity with ligand (**5**), and the reaction profiles are shown in Figure 6. Reaction profiles with both ligands are the same in terms of initial rates and extent of H_2 evolution indicating that making this steric and electronic change had a negligible effect. This was to be expected as catalysis with (**1**) versus (**3**) is also similar in THF. We were also interested in the effect of different Fe(II) precursors and therefore tested $FeBr_2$ (entry 17, Table 1). The overall reaction profile in Figure 6 is the same for both $[Fe(H_2O)_6][BF_4]_2$ and $FeBr_2$ metal precursors, once again suggesting that the same active species is being formed. Both yield the same final amount of H_2 (1.6 equiv in 1 h) although $FeBr_2$ shows a slightly more rapid initial activation, potentially because of improved solubility or more rapid reduction to NPs. To confirm that the activity of $FeBr_2$ with (**5**) can be compared to reactions with (**1**), we also ran reactions using the same substrate loading (Fe:AB = 1:40) as outlined in entry 30 of Table 1 and depicted in Figure 6. Similar initial rates and extent of H_2 evolution at both 1:25 and 1:40 was observed, allowing direct comparisons to be made with (**1**); (**1**) yields 1.1 equiv of H_2 in 30 s, and 1.6 in 1 h, whereas $FeBr_2$ with (**5**) yields 1 equiv in 30 s and 1.4 in 1 h, strongly suggesting the same active site is present in both. Experiments in diglyme (entry 31, Table 1) yield the same results as catalysis in THF for the $FeBr_2$ with (**5**) system, as was observed with (**1**) and (**2**). Manners et al. recently reported the use of skeletal nickel heterogeneous catalysts derived from the selective leaching of aluminum out of a 50/50 Ni/Al alloy for the dehydrogenation of amine-boranes.[29] Although the nickel systems were quite active, similarly prepared iron systems were inactive, suggesting the subtle interplay of metal and stabilizing ligand in our systems which allow them to be so active.

^{11}B NMR analysis of in situ solutions of catalysis with $[Fe(H_2O)_6][BF_4]_2$ and 0.5 equiv of ligand showed two doublets at 30.9 and 27.8 with coupling constants of 127 and 138 Hz respectively. The major species is the doublet at 27.8 ppm, and it appears to have a broad shoulder from 27 to 24 ppm. These peaks correspond closely with those previously observed using (**1**), although the singlets at 20.3 and 24.3 ppm were not

dx.doi.org/10.1021/cs400115p | ACS Catal. 2013, 3, 1092−1102

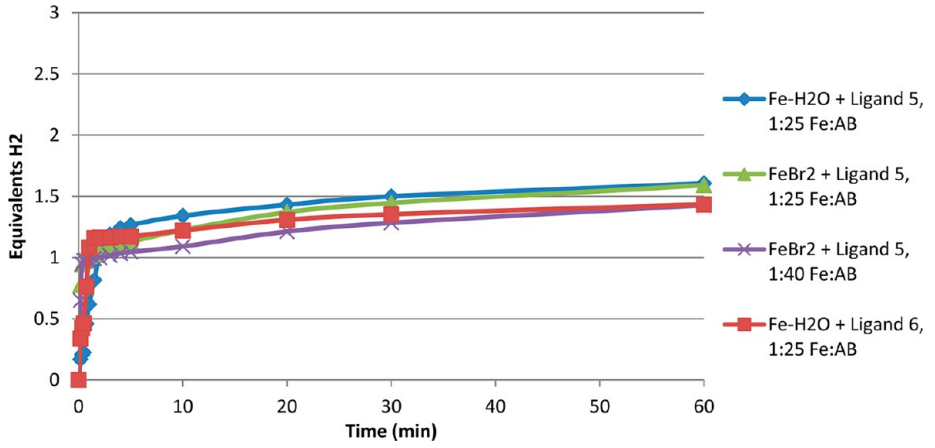

Figure 6. Catalytic dehydrogenation of AB (10 mg, 0.32 mmol) in 5 mL of THF at 22 °C using 4 or 2.5 mol % Fe, 2.6 or 1.6 mol % ligand, and 32 or 20 mol % KOtBu. Fe:Ligand:AB:KOtBu = 1:0.6:25:8 or 1:0.6:40:8. Where Fe−H20 = $[Fe(H_2O)_6][BF_4]_2$.

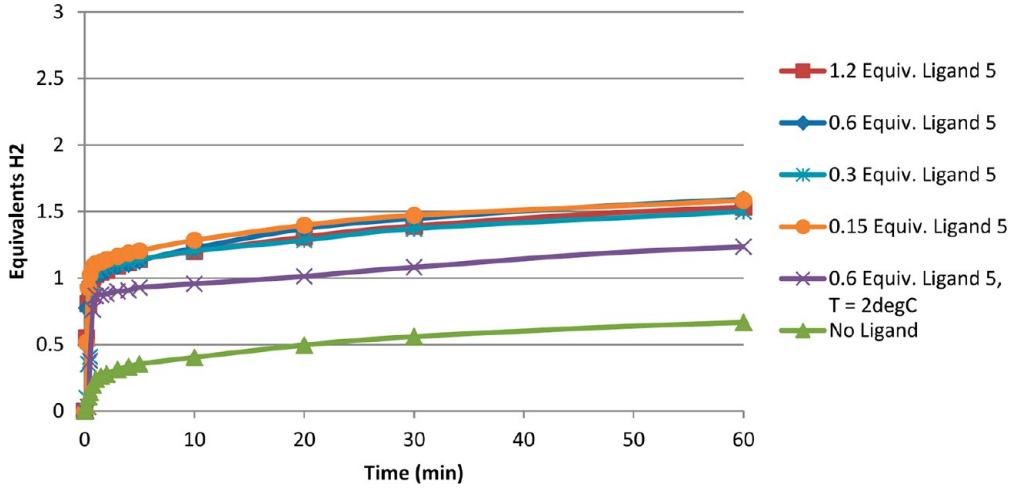

Figure 7. Catalytic dehydrogenation of AB (10 mg, 0.32 mmol) in 5 mL of THF at 22 °C using 4 mol % $FeBr_2$, ligand (**5**) and 32 mol % KOtBu (relative to AB). Fe:AB:KOtBu = 1:25:8.

distinguishable. No peaks for free AB were observed; therefore one would predict from the distribution of products that more than 1.6 equiv of H_2 should have been produced, supporting the theory that deactivation may be caused by binding of reactive B−N intermediates to the active sites of FeNPs, thereby poisoning the catalyst surface. This deactivation mechanism has been previously postulated by Manners et al. on colloidal nickel catalysts.[29] Binding of these species to the surface would make them undetectable by ^{11}B NMR as the NPs would be superparamagnetic.[34]

Using $FeBr_2$ and ligand (**5**), we further probed the temperature dependence of the system by running the reaction at 2 °C as we had done previously with (**1**) (entry 21, Table 1). Similar to the behavior reported with (**1**), the plot at 2 °C shows a similar overall shape as the plot at 22 °C with a slightly slower initial rate, and a deactivation after fewer equivalents of H_2 released (1.2 equiv of H_2 at 2 °C instead of 1.6 at 22 °C). As a second probe to compare the in situ generated catalyst to preformed catalyst we tested $FeBr_2$ and ligand (**5**) for dehydrogenation of AB under an atmosphere of CO. As was observed with (**1**), no hydrogen evolution was observed when the catalyst was generated under a CO atmosphere, indicating that CO impedes catalyst formation in both cases.

Chaudret et al. previously reported[26] a dependence on metal to ligand ratio using their Ru^0 NPs stabilized by 3-amino-propyltriethoxysilane on the initial rates of dehydrogenation of dimethylamineborane (DMAB). We therefore investigated our $FeBr_2$ system with different ratios of ligand (**5**) to determine the effect on stability (extent of conversion prior to deactivation) and initial rates. Figure 7 shows plots of experiments run using 1.2, 0.6, 0.3, and 0.15 equiv of ligand (**5**), relative to $FeBr_2$ (Entries 17−20, Table 1). Plots of 1.2, 0.6, 0.3, and 0.15 equiv of ligand all show the same initial rates of overall conversion, and identical plot shape, yielding 1 equiv of H_2 in 1 min and 1.6 equiv in 1 h. In contrast, the plot shown in green (triangles) represents the addition of no ligand (entry 16, Table 1), and exhibits significantly different behavior. When there is no ligand present, activation is much slower and deactivation occurs much more rapidly, indicating that the ligand provides stabilization on the NP surface preventing agglomeration and active site poisoning. This also suggests that as little as 0.15 equiv of ligand is required to give the needed stabilization to maximize the efficiency of the catalyst. If the catalyst was homogeneous, one would expect to need equimolar amounts of iron and ligand, and that activity would decrease with decreasing ligand amount; however, this is not the case. Further reduction of the amount of ligand yielded irreproducible results and overall decreased activity, indicating

dx.doi.org/10.1021/cs400115p | ACS Catal. 2013, 3, 1092−1102

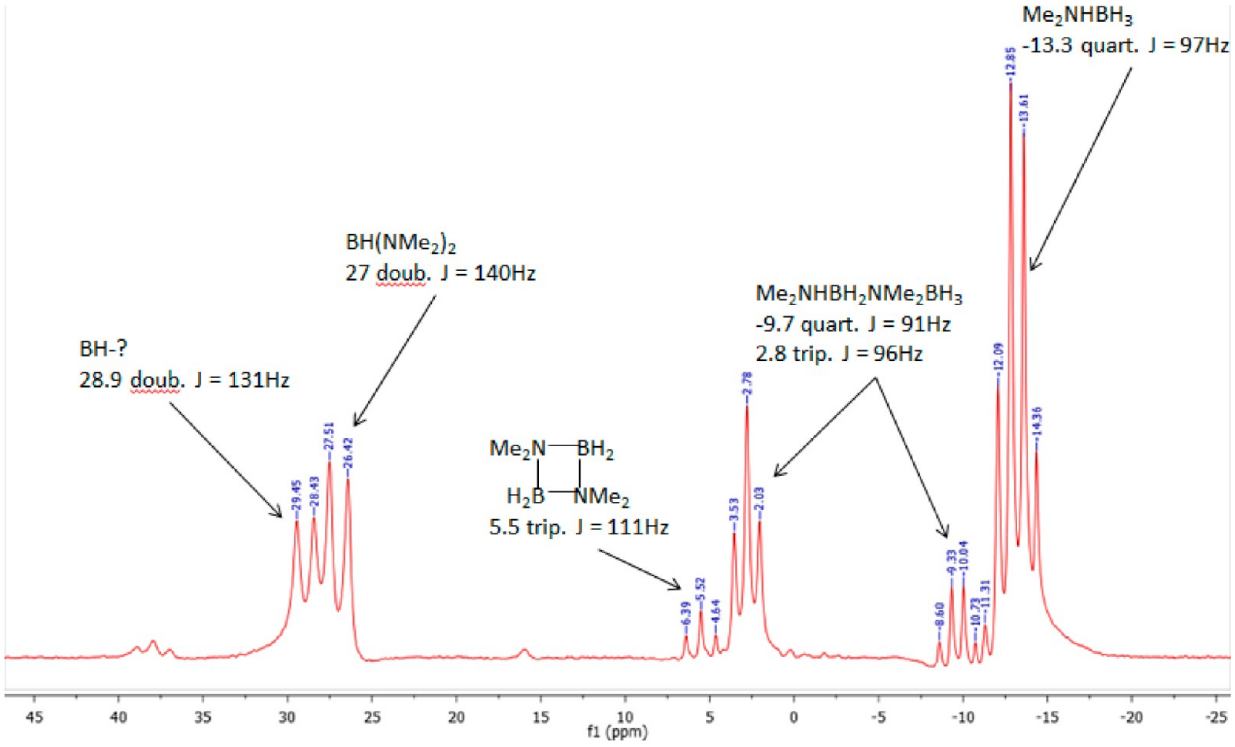

Figure 8. In situ ^{11}B NMR (128 MHz) of catalytic dehydrogenation of Me_2NHBH_3 (entry 24 of Table 1) after 30 min. Fe:B:KOtBu = 1:45:8.

that 0.15 equiv is the minimum amount of ligand necessary for this system. It is interesting that with changing ligand concentration there is no observable effect on the rate of catalysis. Chaudret[26] observed that with too little ligand present larger, less active NPs formed, and this is likely the case with our system, which supports that when <0.15 equiv of ligand are used irreproducible results are obtained. Chaudret also observed that with more ligand present the rate also decreased because of the excess of ligands binding to the active sites. In our system no rate decrease is observed with excess ligand, suggesting that the ligand does not act as an active site poisoning agent, likely because it is fairly bulky. This provides very strong evidence for a heterogeneous system as the active catalyst.

Dimethylamine-borane (DMAB) Dehydrogenation with Precatalysts (1−2). Many heterogeneous precious metal catalysts reported focus primarily on the dehydrogenation of DMAB instead of AB,[16,24,26,28,29,45] and thus we sought to test our systems using (**1**) and (**2**) with KOtBu in THF (Entries 24−25, Table 1). Using the same reaction conditions as employed with AB, and with similar catalyst loading (Fe:KOtBu:DMAB = 1:8:45) hydrogen evolution was measured at 22 °C. (**1**) and (**2**) yielded similar results with (**1**) achieving faster initial rates (0.62 equiv of H_2 in 1 min for (**1**) and 0.44 for (**2**)), but both catalysts yielded 0.97 equiv of H_2 in 1 h and 1.1 equiv in 2 h before deactivation. Similar to the AB plots, dehydrogenation of DMAB shows a rapid initial H_2 evolution, followed by a significant decrease in rate, before complete deactivation of the active species. Addition of more DMAB yielded no further H_2 evolution indicating that catalyst deactivation had occurred, similar to the case with AB. ^{11}B NMR analysis of the reaction solutions proved to be much more complicated than the AB case, and results are depicted in Figure 8. There is a sharp quartet at −13.3 for unreacted DMAB, a triplet at 2.8, and a quartet at −9.7 for the adduct $Me_2NHBH_2NMe_2{\cdot}BH_3$, a small triplet at 5.5 for the $(Me_2N\text{-}BH_2)_2$ heterocycle, which is typically the most common product formed during these reactions as it is the rapid decomposition product of the postulated $Me_2N{=}BH_2$ intermediate.[16,21,29] NMR also shows two doublets at 27 and 28.9 with couplings of 140 and 131 Hz respectively identified as $BH(NMe_2)_2$ and a second BH complex.[22] Given the formation of $BH(NMe_2)_2$ it is likely that BH_3 release occurs, which could interact with $^{-}$OtBu in solution to generate $BH(OtBu)_2$,[46,47] resulting in the doublet found at 28.9 ppm. Given the product distribution, one would surmise that evolution of a full equivalent of H_2 would be unlikely, suggesting that some boron containing products may be insoluble or bound to a superparamagnetic NP, making them undetectable by NMR. This wide range of products and modest yields would suggest that the catalyst is not selective upon reaction with DMAB, nor is it competitive with other reported catalysts, but it is a useful proof of concept for these iron systems and their versatility.

Electron Microscopy Imaging. To further probe the nature of our iron catalytic systems we investigated reaction solutions by transmission electron microscopy (TEM). We analyzed reaction solutions of catalysis with (**1**) and of catalysis with $FeBr_2$ with 0.3 equiv of (**5**) as outlined in entries 28 and 29 respectively of Table 1. Figure 9 [left] is a standard image observed for catalysis with $FeBr_2$ and ligand (**5**) and shows large dense masses with very small dense particles dispersed on the surface. Using energy dispersive X-ray spectroscopy the large masses were identified as KBr, and the small particles were composed of iron. The KBr is formed as a result of decoordination of Br from $FeBr_2$ in the presence of KOtBu. The particles reacted with the electron beam and therefore high magnification imaging was not possible. This indicates that the particles were likely bound to volatile solvent molecules such as THF which were liberated upon exposure to the electron beam. Coordination of THF to FeNPs has been previously reported and supported by extended X-ray absorption fine structure (EXAFS) experiments.[48] This would suggest that the FeNPs generated in situ are stabilized by PNNP ligand and

dx.doi.org/10.1021/cs400115p | ACS Catal. 2013, 3, 1092−1102

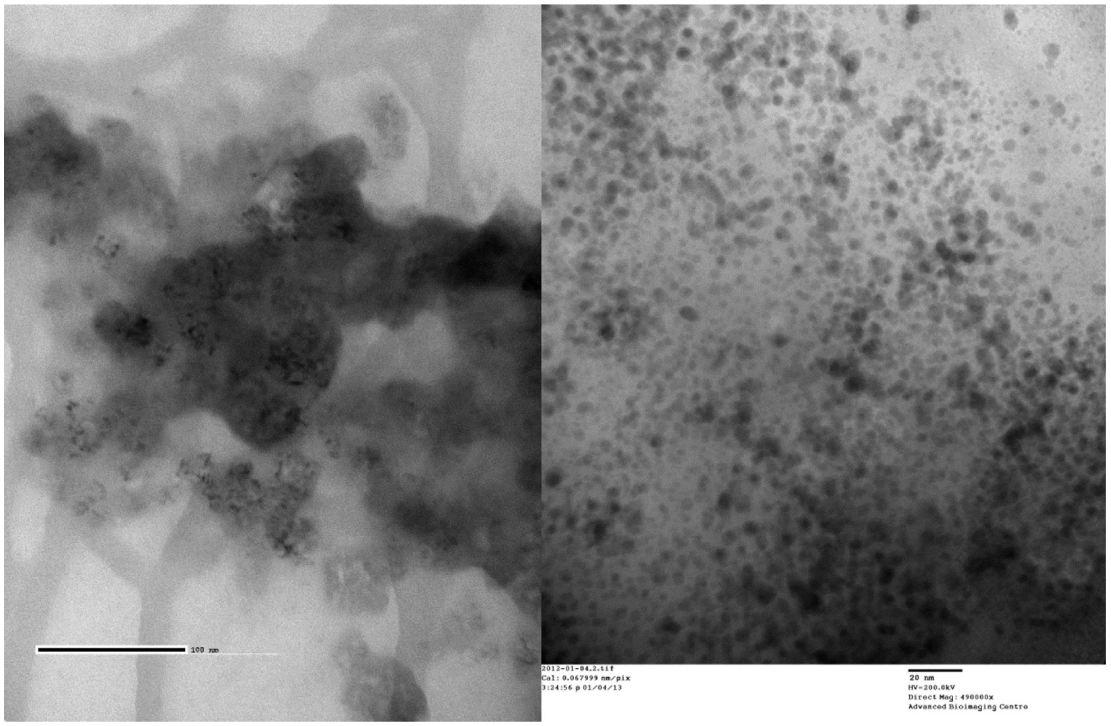

Figure 9. TEM images of entry 29 [left] and entry 28 [right].

THF as a labile ligand, which also supports why the in situ generated catalyst has comparable activity to (**1**) in THF but is more rapidly deactivated in iPrOH. A similar analysis was conducted on catalytic solutions using (**1**). TEM showed dense clusters also identified as potassium salts and dense areas depicted in Figure 9 [right] identified as ∼4 nm FeNPs. Also scattered across the grid were larger (8−12 nm), poorly defined structures of widely varying sizes that were much less dense than the potassium and iron sections of the grid. Using a GIF-2000 energy filter these areas were analyzed for select elements[49] and were determined to be primarily composed of boron. This suggests that the PB identified by ^{11}B NMR is coating the grids, and can be roughly characterized by TEM. Applying a similar energy filter and focusing on phosphorus, it could be shown that phosphorus was primarily bound to the NPs, as would be expected for the ligand. Size distribution analysis using ImageJ software of the FeNPs in Figure 9 [right] indicate that the NPs are 4.1 ± 0.7 nm in diameter, and they appear to be fairly round in shape and moderately well dispersed. This fits within the size range observed for catalysis with (**2**) and (**4**) for TH[34] and also matches closely with the AB dehydrogenation FeNPs reported by Xu et al.[30]

To complete our analysis of these new systems, we were interested in comparing them to our previously explored TH systems.[34] To do this, we generated active catalyst for AB dehydrogenation using our iron precatalysts with AB and KOtBu in THF and then injected these activated solutions into isopropanol solutions containing acetophenone and monitored the conversion to 1-phenylethanol using gas chromatography (GC). Using the GC it is possible to monitor both overall conversion as well as product enantiopurity, so to get the most information out of our catalysis we chose to analyze our two chiral precatalysts (**3**) and (**4**). We previously explained (vide supra) that catalyst deactivation likely occurs during AB dehydrogenation because of the binding of reactive boron compounds to the surface of the NPs. To minimize this deactivation before the catalysts could be used for TH we used less AB for the formation of the active species. A precatalyst to base to AB ratio of 1:7:8 in THF was used to reduce the iron and generate the active species, and this activated solution was injected directly into a vial containing iPrOH and acetophenone, yielding a Fe to ketone ratio of 1:300. Typical TH employing (**4**) and a catalyst to substrate loading of 1:600 yielded 64% ee and 50% conversion in 30 min.[34] Using the systems described herein we achieved 79% ee albeit catalysis took 4 h to reach 50% conversion using (**4**), and no conversion was observed using (**3**). The high enantiopurity indicates that similar to the standard TH case, the chiral ligand must be bound to the surface to induce this level of selectivity.[50,51] The increase in enantiopurity can be attributed to a selectivity enhancement induced by the preference of the system toward preformed catalyst versus in situ generated catalyst, as was observed previously for TH.[34] We hypothesized that the increase in selectivity was due to the unencumbered, complete formation of the ligand-coated nanoparticles without the interference of substrate, allowing for a more optimized coating of the chiral ligand on the surface. The fact that (**4**) and not (**3**) gave active catalysts for TH would indicate that the CO ligand present in precatalyst (**4**) must remain bound to the active species, and that it is necessary for TH. We observed this previously as (**4**) was active for TH and (**3**) was only active for direct hydrogenation.[31] The presence of CO on the active surface therefore plays a critical but not well understood role in catalysis as it slows down AB dehydrogenation, but is crucial for TH. Lastly, it is worth noting the significant decrease in rate on going to the catalysts prepared in THF using KOtBu and AB versus the systems prepared with KOtBu in iPrOH. This rate reduction can likely be attributed to a decrease in catalytic sites caused by the binding of reactive boron containing species to the surface, thereby acting as a catalyst poison. These studies further support that the active species during AB dehydrogenation are FeNPs, similar to those previously investigated.

dx.doi.org/10.1021/cs400115p | *ACS Catal.* 2013, 3, 1092−1102

CONCLUSIONS

We have demonstrated the wide versatility of the series of iron complexes generally described as $[Fe(NCMe)(L)(PPh_2C_6H_4CH{=}NCHR\text{-})_2][BF_4]_2$ for their use in the dehydrogenation of amine-boranes, particularly for ammonia-borane, on top of their efficient previous use as hydrogenation[31,32,34] and oxidation[35] catalysts. In isopropanol, 2.9 equiv of H_2 could be released in under an hour, yielding $B(OiPr)_3$, whereas in nonprotic solvents such as THF and diglyme B−N polymers and oligomers could be formed, and very rapid initial rates were observed yielding turnover frequencies of up to 3.66 H_2/second. Catalysts were shown to be efficient at low temperatures, a quality not previously thoroughly investigated, and were shown to be completely poisoned by carbon monoxide. Electron microscopy imaging showed that iron nanoparticles were forming during catalysis, but could not confirm whether the true catalyst was heterogeneous, or if FeNPs are simply a deactivation product. To probe this property we tested hydrogen evolution using commercially available Fe^{2+} precursors in the presence of varying amounts of PNNP ligand. For a homogeneous catalyst we would expect to need a full equivalent of ligand to achieve comparable activity; however, we have shown that 1.2, 0.6, 0.3, and 0.15 equiv of ligand all achieve the same activity, supporting that the active species are likely to be zerovalent iron nanoparticles coated in, and stabilized by, PNNP ligand, similar to what we observed previously for TH and oxidation with (**2**) and (**4**).[34,35] Although these iron systems still hold many secrets, they have proven themselves to be quite versatile catalysts for a wide range of hydrogen reactions. Given the very rapid initial rates of catalysis it has proven to be quite difficult to run in operando studies to determine the true nature of the catalyst,[52] and we can therefore only propose that the active species are zerovalent iron nanoparticles.

ASSOCIATED CONTENT

Supporting Information

Full experimental details, all catalytic profiles, relevant NMR, electron microscopy images and experiments, kinetic profiles and TH results. This material is available free of charge via the Internet at http://pubs.acs.org.

AUTHOR INFORMATION

Corresponding Author

*E-mail: Robert.Morris@utoronto.ca.

Notes

The authors declare no competing financial interest.

ACKNOWLEDGMENTS

We would like to thank Dr. Doug Holmyard and Dr. Neil Coombs for their invaluable help and expertise with TEM experiments. We would also like to thank the Natural Sciences and Engineering Research Council (NSERC) for a Discovery grant to R.H.M. and for a Canadian Graduate Scholarship and a Vanier Scholarship for J.F.S.

REFERENCES

(1) Dunn, S. *Int. J. Hydrogen Energy* **2002**, *27*, 235.
(2) Schlapbach, L.; Zuttel, A. *Nature* **2001**, *414*, 353.
(3) Cook, T. R.; Dogutan, D. K.; Reece, S. Y.; Surendranath, Y.; Teets, T. S.; Nocera, D. G. *Chem. Rev.* **2010**, *110*, 6474.
(4) Staubitz, A.; Robertson, A. P. M.; Manners, I. *Chem. Rev.* **2010**, *110*, 4079.
(5) Yadav, M.; Xu, Q. *Energy Environ. Sci.* **2012**, *5*, 9698.
(6) Staubitz, A.; Sloan, M. E.; Robertson, A. P. M.; Friedrich, A.; Schneider, S.; Gates, P. J.; Günne, J. r. S.; Manners, I. *J. Am. Chem. Soc.* **2010**, *132*, 13332.
(7) Baker, R. T.; Gordon, J. C.; Hamilton, C. W.; Henson, N. J.; Lin, P.-H.; Maguire, S.; Murugesu, M.; Scott, B. L.; Smythe, N. C. *J. Am. Chem. Soc.* **2012**, *134*, 5598.
(8) Sutton, A. D.; Burrell, A. K.; Dixon, D. A.; Garner, E. B.; Gordon, J. C.; Nakagawa, T.; Ott, K. C.; Robinson, J. P.; Vasiliu, M. *Science* **2011**, *331*, 1426.
(9) Lu, Z.; Conley, B. L.; Williams, T. J. *Organometallics* **2012**, *31*, 6705.
(10) Conley, B. L.; Guess, D.; Williams, T. J. *J. Am. Chem. Soc.* **2011**, *133*, 14212.
(11) Blaquiere, N.; Diallo-Garcia, S.; Gorelsky, S. I.; Black, D. A.; Fagnou, K. *J. Am. Chem. Soc.* **2008**, *130*, 14034.
(12) Denney, M. C.; Pons, V.; Hebden, T. J.; Heinekey, D. M.; Goldberg, K. I. *J. Am. Chem. Soc.* **2006**, *128*, 12048.
(13) Kim, S.-K.; Han, W.-S.; Kim, T.-J.; Kim, T.-Y.; Nam, S. W.; Mitoraj, M.; Piekoś, Ł.; Michalak, A.; Hwang, S.-J.; Kang, S. O. *J. Am. Chem. Soc.* **2010**, *132*, 9954.
(14) Conley, B. L.; Williams, T. J. *Chem. Commun.* **2010**, *46*, 4815.
(15) Käß, M.; Friedrich, A.; Drees, M.; Schneider, S. *Angew. Chem., Int. Ed.* **2009**, *48*, 905.
(16) Sewell, L. J.; Lloyd-Jones, G. C.; Weller, A. S. *J. Am. Chem. Soc.* **2012**, *134*, 3598.
(17) Schreiber, D. F.; O'Connor, C.; Grave, C.; Ortin, Y.; Müller-Bunz, H.; Phillips, A. D. *ACS Catal.* **2012**, *2*, 2505.
(18) Jiang, Y.; Blacque, O.; Fox, T.; Frech, C. M.; Berke, H. *Organometallics* **2009**, *28*, 5493.
(19) Clark, T. J.; Russell, C. A.; Manners, I. *J. Am. Chem. Soc.* **2006**, *128*, 9582.
(20) Keaton, R. J.; Blacquiere, J. M.; Baker, R. T. *J. Am. Chem. Soc.* **2007**, *129*, 1844.
(21) Vogt, M.; de Bruin, B.; Berke, H.; Trincado, M.; Grutzmacher, H. *Chem. Sci.* **2011**, *2*, 723.
(22) Vance, J. R.; Robertson, A. P. M.; Lee, K.; Manners, I. *Chem.—Eur. J.* **2011**, *17*, 4099.
(23) Kawano, Y.; Uruichi, M.; Shimoi, M.; Taki, S.; Kawaguchi, T.; Kakizawa, T.; Ogino, H. *J. Am. Chem. Soc.* **2009**, *131*, 14946.
(24) Jaska, C. A.; Temple, K.; Lough, A. J.; Manners, I. *J. Am. Chem. Soc.* **2003**, *125*, 9424.
(25) Kim, S.-K.; Kim, T.-J.; Kim, T.-Y.; Lee, G.; Park, J. T.; Nam, S. W.; Kang, S. O. *Chem. Commun.* **2012**, *48*, 2021.
(26) Zahmakran, M.; Philippot, K.; Ozkar, S.; Chaudret, B. *Dalton Trans.* **2012**, *41*, 590.
(27) Zahmakiran, M.; Ozkar, S. *Inorg. Chem.* **2009**, *48*, 8955.
(28) Caliskan, S.; Zahmakiran, M.; Durap, F.; Ozkar, S. *Dalton Trans.* **2012**, *41*, 4976.
(29) Robertson, A. P. M.; Suter, R.; Chabanne, L.; Whittell, G. R.; Manners, I. *Inorg. Chem.* **2011**, *50*, 12680.
(30) Yan, J.-M.; Zhang, X.-B.; Han, S.; Shioyama, H.; Xu, Q. *Angew. Chem., Int. Ed.* **2008**, *47*, 2287.
(31) Sui-Seng, C.; Freutel, F.; Lough, A. J.; Morris, R. H. *Angew. Chem., Int. Ed.* **2008**, *47*, 940.
(32) Meyer, N.; Lough, A. J.; Morris, R. H. *Chem.—Eur. J.* **2009**, *15*, 5605.
(33) Prokopchuk, D. E.; Sonnenberg, J. F.; Meyer, N.; Zimmer-De Iuliis, M.; Lough, A. J.; Morris, R. H. *Organometallics* **2012**, *31*, 3056.
(34) Sonnenberg, J. F.; Coombs, N.; Dube, P. A.; Morris, R. H. *J. Am. Chem. Soc.* **2012**, *134*, 5893.
(35) Sonnenberg, J. F.; Pichugin, D.; Coombs, N.; Morris, R. H. *Top. Catal.* **2013**.
(36) Sui-Seng, C.; Haque, F. N.; Hadzovic, A.; Pütz, A. M.; Reuss, V.; Meyer, N.; Lough, A. J.; Zimmer-De Iuliis, M.; Morris, R. H. *Inorg. Chem.* **2009**, *48*, 735.
(37) Gao, J. X.; Zhang, H.; Yi, X. D.; Xu, P. P.; Tang, C. L.; Wan, H. L.; Tsai, K. R.; Ikariya, T. *Chirality* **2000**, *12*, 383.
(38) Mikhailine, A.; Lough, A. J.; Morris, R. H. *J. Am. Chem. Soc.* **2009**, *131*, 1394.

(39) Widegren, J. A.; Finke, R. G. *J. Mol. Catal. A: Chem.* **2003**, *198*, 317.
(40) Crabtree, R. H. *Chem. Rev.* **2012**, *112*, 1536.
(41) Lagaditis, P. O.; Lough, A. J.; Morris, R. H. *Inorg. Chem.* **2010**, *49*, 10057.
(42) Mikhailine, A. A.; Maishan, M. I.; Lough, A. J.; Morris, R. H. *J. Am. Chem. Soc.* **2012**, *134*, 12266.
(43) Prokopchuk, D. E.; Morris, R. H. *Organometallics* **2012**, *31*, 7375.
(44) Watzky, M. A.; Finke, R. G. *J. Am. Chem. Soc.* **1997**, *119*, 10382.
(45) Jaska, C. A.; Temple, K.; Lough, A. J.; Manners, I. *Chem. Commun.* **2001**, 962.
(46) Pelter, A.; Levitt, T. E. *Tetrahedron* **1970**, *26*, 1545.
(47) Onak, T.; Landesman, H.; Williams, R.; Shapiro, I. *J. Phys. Chem.* **1959**, *63*, 1533.
(48) Welther, A.; Bauer, M.; Mayer, M.; Jacobi von Wangelin, A. *ChemCatChem* **2012**, *4*, 1088.
(49) Ahn, C. C.; Krivanek, O. L. *EELS Atlas*; Gatan Inc.: Pleasanton, CA, 1983.
(50) Bönnemann, H.; Braun, G. A. *Angew. Chem., Int. Ed.* **1996**, *35*, 1992.
(51) Osawa, T. *Chem. Lett.* **1985**, 1609.
(52) Bayram, E.; Linehan, J. C.; Fulton, J. L.; Roberts, J. A. S.; Szymczak, N. K.; Smurthwaite, T. D.; Özkar, S.; Balasubramanian, M.; Finke, R. G. *J. Am. Chem. Soc.* **2011**, *133*, 18889.